Adv Comput Math (2022) 48: 44
https://doi.org/10.1007/s10444-022-09937-3

Numerical methods with particular solutions for nonhomogeneous Stokes and Brinkman systems

Carlos J. S. Alves[1] · **Nuno F. M. Martins**[2] · **Ana L. Silvestre**[1]

Received: 8 April 2021 / Accepted: 24 February 2022 / Published online: 2 July 2022

Abstract

This paper deals with the numerical approximation of solutions of Stokes and Brinkman systems using meshless methods. The aim is to solve a problem containing a nonzero body force, starting from the well known decomposition in terms of a particular solution and the solution of a homogeneous force problem. We propose two methods for the numerical construction of a particular solution. One method is based on the Neuber-Papkovich potentials, which we extend to nonhomogeneous Brinkman problems. A second method relies on a Helmholtz-type decomposition for the body force and enables the construction of divergence-free basis functions. Such basis functions are obtained from Hänkel functions and justified by new density results for the space $H^1(\Omega)$. Several 2D numerical experiments are presented in order to discuss the feasibility and accuracy of both methods.

Keywords Meshfree method · Fundamental solutions · Nonhomogeneous Brinkman equations · Nonhomogeneous Stokes equations · Particular solutions · Density theorems

Mathematics Subject Classification (2010) 35J25 · 35Q35 · 65N38 · 65N80 · 76D07

Communicated by: Gianluigi Rozza

✉ Nuno F. M. Martins
nfm@fct.unl.pt

Carlos J. S. Alves
carlos.alves@math.tecnico.ulisboa.pt

Ana L. Silvestre
ana.silvestre@math.tecnico.ulisboa.pt

[1] Department of Mathematics and CEMAT, Instituto Superior Técnico, Universidade de Lisboa, Lisbon, Portugal

[2] Department of Mathematics, FCT-NOVA, Almada, Portugal

1 Introduction

Fundamental solutions methods and singularity methods [21] for boundary value problems involving PDEs became popular due to their easy computational implementation and the fact that they allow a smooth representation of the solution inside the domain of interest. Compared to other methods, elaborate discretizations on the boundary and numerical integrations are avoided, and the evaluation of the approximate solution and its derivatives at interior points of the domain can be carried out directly. Moreover, a posteriori error estimates can be computed based on the estimates for the continuous problem. The drawback of such methods is the requirement of fundamental solutions adapted to a linear PDE, and ultimately, the numerical resolution of linear systems which can be severely ill-conditioned (e.g. [7] for an overview).

The application of the method of fundamental solutions (MFS) to linear homogeneous source/force problems is well known (e.g. [5]). When solving nonhomogeneous source/force problems, nonlinear or time-dependent problems, it is necessary to find a particular solution and then, the problem can be reduced to the application of the MFS. Several approaches have been proposed for deriving approximate particular solutions, among them, the so-called domain method of fundamental solutions (MFS-D) [2]. This method is based on a set of frequencies and point-sources that lead to an extended MFS that approximates a L^2-function in a bounded domain. For a general overview of state of the art of meshless methods, we refer to [18]. Convergence results are available for Laplace's and Poisson's equation in $\mathbb{R}^2$ in specific geometries, like disks [10, 13, 19]. The stability and convergence of the MFS for Helmholtz problems are studied in [4].

MFS techniques have been partially applied for the computational approximation of solutions of the Stokes equations (e.g. [23, 25]), and of Navier-Stokes equations (e.g. [16, 27]). For a recent application of the MFS to the Oseen equations see [11].

In this paper we consider nonhomogeneous Stokes/Brinkman problems and provide a mathematical justification for MFS approaches based on density results that justify the approximation on the boundary data and in the domain for $\mathbf{L}^2$ body forces. This work extends previous different results [3, 14] on the application of the MFS to Stokes and Brinkman equations [6, 12].

Let $\Omega \subset \mathbb{R}^d$, $d = 2, 3$ be an open, bounded, simply connected set with Lipschitz boundary $\Gamma = \partial\Omega$ and consider the following Stokes/Brinkman system with Dirichlet boundary condition

$$\begin{cases} -(\Delta - \kappa)\mathbf{u} + \nabla p = \mathbf{f} \text{ in } \Omega, & \kappa \geq 0, \\ \nabla \cdot \mathbf{u} = 0 & \text{in } \Omega \\ \mathbf{u} = \mathbf{g} & \text{on } \Gamma \end{cases} \tag{1}$$

with body force $\mathbf{f} \in \mathbf{L}^2(\Omega) = (L^2(\Omega))^d$ and boundary data $\mathbf{g} \in \mathbf{H}_{\mathbf{n}}^{\frac{1}{2}}(\Gamma)$, where

$$\mathbf{H}_{\mathbf{n}}^{\frac{1}{2}}(\Gamma) = \left\{ \mathbf{g} \in H^{\frac{1}{2}}(\Gamma)^d : \int_\Gamma \mathbf{g}(\mathbf{x}) \cdot \mathbf{n}(\mathbf{x}) dS_{\mathbf{x}} = 0 \right\}$$

and $\mathbf{n}(\mathbf{x})$ is the normal vector field at $\mathbf{x} \in \Gamma$, pointing outwards with respect to Ω. Under these conditions, there exists a velocity and pressure $(\mathbf{u}, p) \in \mathbf{H}^1(\Omega) \times L^2(\Omega)$ solving problem (1), unique up to a constant for the pressure. The constant is uniquely determined by considering

$$p \in L_0^2(\Omega) = \left\{ p \in L^2(\Omega) : \int_\Omega p(\mathbf{x}) d\mathbf{x} = 0 \right\}.$$

The solution $(\mathbf{u}, p)$ of problem (1) will be decomposed as

$$(\mathbf{u}, p) = (\mathbf{u}_{\text{part}}, p_{\text{part}}) + (\mathbf{u}_{\text{hom}}, p_{\text{hom}})$$

where $(\mathbf{u}_{\text{part}}, p_{\text{part}})$ is a particular solution,

$$\begin{cases} -(\Delta - \kappa)\mathbf{u}_{\text{part}} + \nabla p_{\text{part}} = \mathbf{f} & \text{in } \Omega \\ \nabla \cdot \mathbf{u}_{\text{part}} = \mathbf{0} & \text{in } \Omega \end{cases} \tag{2}$$

and $(\mathbf{u}_{\text{hom}}, p_{\text{hom}})$ satisfies the homogeneous boundary value problem

$$\begin{cases} -(\Delta - \kappa)\mathbf{u}_{\text{hom}} + \nabla p_{\text{hom}} = \mathbf{0} & \text{in } \Omega \\ \nabla \cdot \mathbf{u}_{\text{hom}} = \mathbf{0} & \text{in } \Omega \\ \mathbf{u}_{\text{hom}} = \mathbf{g} - \mathbf{u}_{\text{part}} & \text{on } \Gamma. \end{cases} \tag{3}$$

The first method that we propose is based on the Neuber-Papkovich potentials [17, 20, 24], which we extend to nonhomogeneous Brinkman problems (2). Such potentials can be numerically computed using the approach of [2] for Helmholtz and Poisson problems.

Starting from a new theoretical density result for the space $H^1(\Omega)$, namely Theorem 1, another method is proposed for $(\mathbf{u}_{\text{part}}, p_{\text{part}})$ which relies on a Helmholtz-type decomposition for the forcing term $\mathbf{f}$ and has the advantage of yielding divergence-free basis functions, see Propositions 1 and 2.

The plan of the paper is the following. In Section 2, we prove new density results for the Sobolev space $H^1(\Omega)$, where $\Omega \subset \mathbb{R}^d$ is a bounded domain. Concerning $(\mathbf{u}_{\text{part}}, p_{\text{part}})$, the generalization of the Neuber-Papkovich potentials is presented in Section 3. In Section 4, based on the results of Section 2, divergence-free basis functions are given explicitly in dimensions $d = 2$ and $d = 3$, together with the algorithm for the associated MFS-D. Section 5 recalls the MFS algorithm to find $(\mathbf{u}_{\text{hom}}, p_{\text{hom}})$. Several numerical experiments to illustrate the proposed methods for the Brinkman system are presented in Section 6. Conclusions are summarized in Section 7.

2 New density results

Here, we prove two density results for the space $H^1(\Omega)$ which will be used in the next sections, namely to define the basis functions in the proposed numerical approaches. In what follows, $\mathbb{S}^{d-1}$ stands for the boundary of the hypersphere in dimension d.

Lemma 1 *The set of trigonometric polynomials*

$$\mathcal{S} := \left\{ e^{i\kappa \mathbf{x}\cdot\xi}|_{\mathbf{x}\in\Omega} : \xi \in \mathbb{S}^{d-1}, \kappa \in I =]a, b[\subseteq \mathbb{R}^+ \right\}$$

spans a dense subspace in $H^1(\Omega)$.

Proof Set $s_\kappa(x) := e^{\mathrm{i}\kappa \mathbf{x}\cdot\xi}$. Suppose $\mathcal{S} \subset \mathrm{Ker}(L)$ for some $L \in H^1(\Omega)'$, that is

$$\langle L, s_\kappa \rangle_{H^1(\Omega)', H^1(\Omega)}(\xi) = 0, \quad \forall \xi \in \mathbb{S}^{d-1}, \ \forall \kappa \in I.$$

Using the characterisations (see, for example [15] and [8, pg. 283, Theorem 1])

$$H^1(\Omega)' = \tilde{H}^{-1}(\Omega) = \{U|_\Omega : U \in H^{-1}(\mathbb{R}^d), \ \mathrm{supp}\, U \subseteq \overline{\Omega}\},$$

and

$$\begin{aligned} H^{-1}(\mathbb{R}^d) &= H_0^1(\mathbb{R}^d)' \\ &= \left\{ U \in \mathcal{D}'(\mathbb{R}^d) : U = f_0 + \sum_{i=1}^{d} \frac{\partial f_i}{\partial x_i}, \ f_i \in L^2(\mathbb{R}^d) \ (i = 0, 1, ..., d) \right\}, \end{aligned}$$

we take $U \in H_0^1(\mathbb{R}^d)'$ such that $\mathrm{supp}\, U \subseteq \overline{\Omega}$ and $L = U|_\Omega$. More specifically, the functions f_0, f_1,..., $f_d \in L^2(\mathbb{R}^d)$ used for the representation of U have compact support contained in $\overline{\Omega}$. Hence, U is a distribution of compact support, $U \in \mathcal{E}'(\mathbb{R}^d) \subset \mathcal{S}'(\mathbb{R}^d)$, which satisfies ($\mathcal{F}$ here stands for the Fourier transform)

$$\begin{aligned} \mathcal{F}(U)(-\kappa\xi) &= \langle U, s_\kappa \rangle_{\mathcal{E}'(\mathbb{R}^d), \mathcal{E}(\mathbb{R}^d)}(\xi) \\ &= \langle L, s_\kappa \rangle_{H^1(\Omega)', H^1(\Omega)}(\xi) = 0, \ \forall \xi \in \mathbb{S}^{d-1}, \ \forall \kappa \in I. \end{aligned}$$

We conclude that $\mathcal{F}(U)(y) = 0$ for all $y \in B(0, b) \setminus \overline{B(0, a)}$. Since the Fourier transform of a compactly supported distribution is analytic, it follows that $\mathcal{F}(U) \equiv 0$ and therefore, $L \equiv 0$. □

Next, we deduce a density result for $H^1(\Omega)$ based on the fundamental solution of the Helmholtz's equation

$$-(\Delta + \kappa) H_\kappa = \delta, \ \text{in } \mathbb{R}^d \quad (\kappa > 0)$$

thus extending the result for $L^2(\Omega)$ proved in [2]. Similar results can be proved based on the fundamental solution of the modified Helmholtz's equation.

It is convenient to recall a number of special functions, for which a classical reference is [1]. For $\alpha \in \mathbb{R}$, J_α and Y_α represent the Bessel functions of the first kind and second kind, respectively,

$$J_\alpha(z) = \left(\frac{z}{2}\right)^\alpha \sum_{k=0}^{\infty} \frac{(-1)^k}{k!} \frac{\left(\frac{z}{2}\right)^{2k}}{\Gamma(\alpha + k + 1)} \quad (z \in \mathbb{C}),$$

where Γ denotes the gamma function, and

$$Y_\alpha(z) = \frac{J_\alpha(z)\cos(\alpha\pi) - J_{-\alpha}(z)}{\sin(\alpha\pi)}.$$

The Hankel functions of the first kind are defined as

$$H_\alpha^{(1)}(z) = J_\alpha(z) + \mathrm{i} Y_\alpha(z),$$

in particular, we have

$$H^{(1)}_{1/2}(z) = \sqrt{\frac{2}{\pi z}}\frac{\exp(\mathrm{i}z)}{\mathrm{i}}.$$

The fundamental solution of the Helmholtz equation is given by

$$H_\kappa(\mathbf{x}) = \frac{\mathrm{i}}{4}\left(\frac{\sqrt{k}}{2\pi|\mathbf{x}|}\right)^{d/2-1} H^{(1)}_{d/2-1}(\sqrt{k}|\mathbf{x}|), \tag{4}$$

where $|\mathbf{x}|$ is the Euclidian norm of $\mathbf{x} \in \mathbb{R}^d \setminus \{0\}$. We will need the specific cases

$$H_\kappa(\mathbf{x}) = \begin{cases} \frac{\mathrm{i}}{4}H^{(1)}_0(\sqrt{k}|\mathbf{x}|), & when\ d = 2 \\ \frac{\exp(-\mathrm{i}\sqrt{\kappa}|\mathbf{x}|)}{4\pi|\mathbf{x}|}, & when\ d = 3. \end{cases}$$

Before stating and proving the density result, we consider the problem

$$-\kappa\int_\Omega uv dx + \int_\Omega \nabla u\cdot\nabla v dx = \langle L, v\rangle_{H^1(\Omega)',H^1(\Omega)},\ \forall v \in H^1(\Omega), \tag{5}$$

where $\kappa > 0$ and recall that there exists an at most countable set $\mathcal{C} \subset \mathbb{R}$ such that the problem (5) has a unique solution for each $L \in H^1(\Omega)'$ if and only if $\kappa \notin \mathcal{C}$.

Theorem 1 *Let $I =]a, b[\subseteq \mathbb{R}^+ \setminus \mathcal{C}$ and $\hat{\Gamma} = \partial\hat{\Omega}$, with $\bar{\Omega} \subset \hat{\Omega}$, an artificial boundary of Ω. The set*

$$\mathcal{W} := \left\{ H_\kappa(\cdot - \mathbf{y})|_\Omega : \mathbf{y} \in \hat{\Gamma},\ \kappa \in I \right\}$$

spans a dense subspace in $H^1(\Omega)$.

Proof Suppose $\mathcal{W} \subset \mathrm{Ker}(L)$ for some $L \in H^1(\Omega)'$, that is,

$$\langle L, H_\kappa(\cdot - \mathbf{y})\rangle_{H^1(\Omega)',H^1(\Omega)} = 0,\ \forall(\mathbf{y},\kappa) \in \hat{\Gamma}\times I. \tag{6}$$

For each $\kappa \in I$, let $u^{\mathrm{int}}_\kappa \in H^1(\Omega)$ be the unique solution of the interior problem

$$-\kappa\int_\Omega u^{\mathrm{int}}_\kappa v dx + \int_\Omega \nabla u^{\mathrm{int}}_\kappa\cdot\nabla v dx = \langle L, v\rangle_{H^1(\Omega)',H^1(\Omega)},\ \forall v \in H^1(\Omega). \tag{7}$$

If we take $v = H_\kappa(\cdot - \mathbf{y})$ ($\mathbf{y} \in \hat{\Gamma}$) in (7), it follows from (6) that

$$-\kappa\int_\Omega u^{\mathrm{int}}_\kappa(\mathbf{x})H_\kappa(\mathbf{x}-\mathbf{y})d\mathbf{x} + \int_\Omega \nabla u^{\mathrm{int}}_\kappa(\mathbf{x})\cdot\nabla H_\kappa(\mathbf{x}-\mathbf{y})d\mathbf{x} = 0,\ \forall(\mathbf{y},\kappa) \in \hat{\Gamma}\times I.$$

Using the relation $(\Delta + \kappa)H_\kappa(\mathbf{x}-\mathbf{y}) = 0$, for $\mathbf{x} \in \Omega$ and $\mathbf{y} \in \hat{\Gamma}$, and integration by parts

$$\begin{aligned} -\kappa\int_\Omega u^{\mathrm{int}}_\kappa(\mathbf{x})H_\kappa(\mathbf{x}-\mathbf{y})d\mathbf{x} &= \int_\Omega u^{\mathrm{int}}_\kappa(\mathbf{x})\Delta H_\kappa(\mathbf{x}-\mathbf{y})d\mathbf{x} = \\ &= \int_{\partial\Omega} u_\kappa(\mathbf{x})\frac{\partial H_\kappa(\mathbf{x}-\mathbf{y})}{\partial\mathbf{n}}dS_\mathbf{x} - \int_\Omega \nabla u^{\mathrm{int}}_\kappa(\mathbf{x})\nabla H_\kappa(\mathbf{x}-\mathbf{y})d\mathbf{x} \end{aligned}$$

yields

$$\int_\Gamma u^{\mathrm{int}}_\kappa(\mathbf{x})\frac{\partial H_\kappa(\mathbf{x}-\mathbf{y})}{\partial\mathbf{n}}dS_\mathbf{x} = 0,\quad \forall(\mathbf{y},\kappa) \in \hat{\Gamma}\times I.$$

Now, consider the trace $u_\kappa(\mathbf{x}) := u_\kappa^{\text{int}}|_\Gamma(\mathbf{x})$ in $H^{1/2}(\Gamma)$ and the double layer representation

$$w_\kappa(\mathbf{y}) := -\int_\Gamma u_\kappa(\mathbf{x}) \frac{\partial H_\kappa(\mathbf{x}-\mathbf{y})}{\partial \mathbf{n}} dS_{\mathbf{x}} \quad (\mathbf{y} \in \mathbb{R}^d \setminus \Gamma). \tag{8}$$

Define $w_\kappa^{\text{ext}} := w_\kappa|_{\overline{\Omega}^c}$ and $w_\kappa^{\text{int}} := w_\kappa|_\Omega$.
Since w_κ^{ext} satisfies

$$\begin{cases} -(\Delta+\kappa)w_\kappa^{\text{ext}} = 0, \text{ in } \overline{\Omega}^c, \\ \partial_r w_\kappa^{\text{ext}}(\mathbf{y}) - \mathrm{i}\sqrt{\kappa} w_\kappa^{\text{ext}}(\mathbf{y}) = \mathrm{o}(r^{(1-d)/2}), \quad r = |\mathbf{y}| \end{cases}$$

and $w_\kappa^{\text{ext}}(\mathbf{y}) = 0$, for $\mathbf{y} \in \hat{\Gamma}$, we have

$$\begin{cases} -(\Delta+\kappa)w_\kappa^{\text{ext}} = 0, \text{ in } \overline{\hat{\Omega}}^c, \\ w_\kappa^{\text{ext}} = 0, \text{ on } \hat{\Gamma}, \\ \partial_r w_\kappa^{\text{ext}}(\mathbf{y}) - \mathrm{i}\sqrt{\kappa} w_\kappa^{\text{ext}}(\mathbf{y}) = \mathrm{o}(r^{(1-d)/2}). \end{cases}$$

By well-posedness of the exterior Dirichlet problem for the Helmholtz equation, we conclude that $w_\kappa^{\text{ext}} \equiv 0$ in $\hat{\Omega}^c$ (the complementary set of $\hat{\Omega}$). By analytic continuation, w_κ^{ext} can be extended to $\overline{\Omega}^c$ as $w_\kappa^{\text{ext}} \equiv 0$.

Now, the double layer representation (8) implies that the normal trace $\frac{\partial w_\kappa^{\text{int}}}{\partial \mathbf{n}}$ on Γ is null and since $-(\Delta+\kappa)w_\kappa^{\text{int}} = 0$ in Ω and $\kappa \notin \mathcal{C}$ then $w_\kappa^{\text{int}} = 0$ in Ω and thus

$$w_\kappa^{\text{int}}|_{\partial\Omega} = u_\kappa \equiv 0 \text{ on } \Gamma. \tag{9}$$

To complete the proof, take $v(\mathbf{x}) = s^{\sqrt{\kappa}}(\mathbf{x}) = e^{\mathrm{i}\sqrt{\kappa}\xi\cdot\mathbf{x}}$ (with $\xi \in \mathbb{S}^{d-1}$, $\kappa \in I$ as in Lemma 1) in the variational formulation (7):

$$-\kappa \int_\Omega u_\kappa^{\text{int}} s^{\sqrt{\kappa}} d\mathbf{x} + \int_\Omega \nabla u_\kappa^{\text{int}} \cdot \nabla s^{\sqrt{\kappa}} d\mathbf{x} = \langle L, s^{\sqrt{\kappa}} \rangle_{H^1(\Omega)', H^1(\Omega)}.$$

Since $(\Delta+\kappa)s^{\sqrt{\kappa}} = 0$, we get, using (9),

$$-\kappa \int_\Omega u_\kappa^{\text{int}} s^{\sqrt{\kappa}} d\mathbf{x} = \int_\Omega u_\kappa^{\text{int}} \Delta s^{\sqrt{\kappa}} d\mathbf{x} =$$

$$\int_\Gamma u_\kappa \frac{\partial s^{\sqrt{\kappa}}}{\partial \mathbf{n}} dS - \int_\Omega \nabla u_\kappa^{\text{int}} \cdot \nabla s^{\sqrt{\kappa}} d\mathbf{x} = -\int_\Omega \nabla u_\kappa^{\text{int}} \cdot \nabla s^{\sqrt{\kappa}} d\mathbf{x}.$$

From (7) and

$$-\kappa \int_\Omega u_\kappa^{\text{int}} s^{\sqrt{\kappa}} d\mathbf{x} + \int_\Omega \nabla u_\kappa^{\text{int}} \cdot \nabla s^{\sqrt{\kappa}} d\mathbf{x} = 0$$

it follows

$$\langle L, s^{\sqrt{\kappa}} \rangle_{H^1(\Omega)', H^1(\Omega)} = 0, \quad \forall \kappa \in I,\ \xi \in \mathbb{S}^{d-1},$$

and by the density result for $H^1(\Omega)$ of Lemma 1, we conclude that $L \equiv 0$. Therefore, $\mathcal{W}$ is dense in $H^1(\Omega)$. □

In the next section, the above density results will be used to tackle the numerical computation of a particular solution.

3 Numerical method based on Neuber-Papkovich potentials

In this section, we extend the Neuber-Papkovich decomposition to the Stokes and Brinkman systems with nonhomogeneous forcing terms and use this tool to obtain particular solutions $(\mathbf{u}_{\text{part}}, p_{\text{part}})$ for the such systems.

3.1 Neuber-Papkovich decomposition

For $\mathbf{f} \in \mathbf{L}^2(\Omega)$, let $(\Psi, \psi) \in \mathbf{H}^2(\Omega) \times H^2(\Omega)$ satisfy the following modified Helmholtz and Poisson problems (the regularity is ensured by [8, pgs. 309,317], eventually taking a C^2 domain larger than $\bar{\Omega}$ to solve a boundary value problem with an L^2-extension of $\mathbf{f}$ or using the whole space and an L^2-extension of $\mathbf{f}$)

$$\begin{cases} -(\Delta - \kappa)\Psi = \frac{1}{2}\mathbf{f}, \\ -\Delta\psi = \kappa\mathbf{x}\cdot\Psi - \frac{1}{2}\mathbf{x}\cdot\mathbf{f}, \text{ in } \Omega \end{cases} \tag{10}$$

and define

$$\mathbf{u}_{\text{part}} = 2\Psi - \nabla(\mathbf{x}\cdot\Psi + \psi), \quad p_{\text{part}} = \kappa(\mathbf{x}\cdot\Psi + \psi) - 2\nabla\cdot\Psi. \tag{11}$$

Then, $\mathbf{u}_{\text{part}}$ is a solenoidal vector field,

$$\begin{aligned} \nabla\cdot\mathbf{u}_{\text{part}} &= 2\nabla\cdot\Psi - \Delta(\mathbf{x}\cdot\Psi + \psi) = 2\nabla\cdot\Psi - \mathbf{x}\cdot\Delta\Psi - 2\nabla\cdot\Psi - \Delta\psi \\ &= -(\Delta\psi + \mathbf{x}\cdot\Delta\Psi) = 0 \text{ in } \Omega. \end{aligned}$$

Furthermore,

$$\nabla p_{\text{part}} = \kappa\nabla(\mathbf{x}\cdot\Psi + \psi) - 2\nabla(\nabla\cdot\Psi) = 2\kappa\Psi - \kappa\mathbf{u}_{\text{part}} - 2\nabla(\nabla\cdot\Psi),$$

$$\begin{aligned} \Delta\mathbf{u}_{\text{part}} &= \Delta(2\Psi - \nabla(\mathbf{x}\cdot\Psi + \psi)) = 2\Delta\Psi - \nabla(\Delta(\mathbf{x}\cdot\Psi)) + \Delta\psi) \\ &= 2\Delta\Psi - \nabla(\mathbf{x}\cdot\Delta\Psi + \Delta\psi) - 2\nabla(\nabla\cdot\Psi) = 2\Delta\Psi - 2\nabla(\nabla\cdot\Psi) \\ &= 2\kappa\Psi - \mathbf{f} + \nabla p_{\text{part}} + \kappa\mathbf{u}_{\text{part}} - 2\kappa\Psi = \nabla p_{\text{part}} + \kappa\mathbf{u}_{\text{part}} - \mathbf{f} \end{aligned}$$

so that

$$-\Delta\mathbf{u}_{\text{part}} + \kappa\mathbf{u}_{\text{part}} + \nabla p_{\text{part}} = \mathbf{f} \text{ in } \Omega.$$

3.2 Numerical method using Neuber-Papkovich potentials

In order to obtain a particular solution based on the Neuber-Papkovich decomposition (11), we will use system (10) or

$$\begin{cases} -(\Delta - \kappa)\Psi = \frac{1}{2}\mathbf{f}, \\ -\Delta\psi = \mathbf{x}\cdot\Delta\Psi, \text{ in } \Omega. \end{cases}$$

along with the density result of Lemma 1.

In the first step of the method, we consider the following approximation for the vector potential Ψ:

$$\tilde{\Psi}(\mathbf{x}) = \sum_{k=1}^{M}\sum_{l=1}^{N} \frac{\alpha^{(k,l)}}{\lambda_k^2 + \kappa} e^{\mathrm{i}\lambda_k\mathbf{x}\cdot\mathbf{d}^{(l)}}, \quad \kappa \neq \lambda_k \in \Sigma \subset \mathbb{R}^+, \quad \mathbf{d}^{(l)} \in S \subset \mathbb{S}^{d-1}, \tag{12}$$

where Σ is a set of frequencies, S a set of directions and $\alpha^{(k,l)} = (\alpha_1^{(k,l)}, \ldots, \alpha_d^{(k,l)}) \in \mathbb{C}^d$ are $k \times l$ vector coefficients which will be computed by imposing

$$-(\Delta - \kappa)\tilde{\Psi}(\mathbf{x}^{(j)}) = \sum_{k=1}^{M}\sum_{l=1}^{N} \alpha^{(k,l)} e^{\mathrm{i}\lambda_k \mathbf{x}^{(j)}\cdot\mathbf{d}^{(l)}} = \frac{1}{2}\mathbf{f}(\mathbf{x}^{(j)}) \tag{13}$$

where $\mathbf{x}^{(j)} \in \tilde{\Omega}, \quad j = 1, \ldots, K$, are collocation points placed at a domain $\tilde{\Omega}$ containing Ω. After solving this problem for $\tilde{\Psi}$, we consider the following approximation for the scalar potential ψ

$$\tilde{\psi}(\mathbf{x}) = \sum_{k=1}^{M}\sum_{l=1}^{N} \frac{\beta^{(k,l)}}{\lambda_k^2} e^{\mathrm{i}\lambda_k \mathbf{x}\cdot\mathbf{d}^{(l)}}, \tag{14}$$

where, for simplicity, we have considered the same set of frequencies Σ and directions S used in (12). Analogously, we compute the coefficients $\beta^{(k,l)}$ by imposing

$$-\Delta\tilde{\psi}(\mathbf{x}^{(j)}) = \sum_{k=1}^{M}\sum_{l=1}^{N} \beta^{(k,l)} e^{\mathrm{i}\lambda_k \mathbf{x}^{(j)}\cdot\mathbf{d}^{(l)}} = \mathbf{x}^{(j)} \cdot \Delta\tilde{\Psi}(\mathbf{x}^{(j)}), \tag{15}$$

with the same collocation points $\mathbf{x}^{(j)}$ considered above in (13).

Concerning the computation of the coefficients $\alpha^{(k,l)}$ and $\beta^{(k,l)}$ of $\tilde{\Psi}$ and $\tilde{\psi}$, we define

$$A = \begin{bmatrix} e^{\mathrm{i}\lambda_1 \mathbf{x}^{(1)}\cdot\mathbf{d}^{(1)}} & \cdots & e^{\mathrm{i}\lambda_M \mathbf{x}^{(1)}\cdot\mathbf{d}^{(N)}} \\ \vdots & \ddots & \vdots \\ e^{\mathrm{i}\lambda_1 \mathbf{x}^{(K)}\cdot\mathbf{d}^{(1)}} & \cdots & e^{\mathrm{i}\lambda_M \mathbf{x}^{(K)}\cdot\mathbf{d}^{(N)}} \end{bmatrix}_{K\times(M\times N)}$$

and the equations corresponding to the second identities in (13) and (15) can be written as

$$AX_i = B_i, \ \imath = 1, \ldots, d, \quad AY = C, \tag{16}$$

where

$$X_i = \begin{bmatrix} \alpha_i^{(k,l)} \end{bmatrix}_{(M\times N)\times 1}, \quad B_i = \frac{1}{2}\begin{bmatrix} f_i(\mathbf{x}^{(1)}) \\ \vdots \\ f_i(\mathbf{x}^{(K)}) \end{bmatrix}_{K\times 1}, \quad i = 1, ..., d,$$

$$Y = \begin{bmatrix} \beta^{(k,l)} \end{bmatrix}_{(M\times N)\times 1}, \quad C = \begin{bmatrix} \mathbf{x}^{(1)} \cdot \Delta\tilde{\Psi}(\mathbf{x}^{(1)}) \\ \vdots \\ \mathbf{x}^{(K)} \cdot \Delta\tilde{\Psi}(\mathbf{x}^{(K)}) \end{bmatrix}_{K\times 1}.$$

Note that, by considering the same basis functions in (12) and (14), the same collocation points, directions and frequencies, this method requires the construction of only one matrix, the matrix A, leading to a more efficient scheme.

Once system (16) is solved and the coefficients $\alpha_i^{(k,l)}$, $i = 1, ..., d$, and $\beta^{(k,l)}$ of $\tilde{\Psi}$ and $\tilde{\psi}$ are available, based on (11), we obtain the following approximation for the particular solution

$$\tilde{\mathbf{u}}_{\text{part}} = 2\tilde{\Psi} - \nabla(\mathbf{x}\cdot\tilde{\Psi} + \tilde{\psi}), \quad \tilde{p}_{\text{part}} = \kappa(\mathbf{x}\cdot\tilde{\Psi} + \tilde{\psi}) - 2\nabla\cdot\tilde{\Psi}.$$

Remark 1 We write the approximating vector potential $\tilde{\Psi}$ as

$$-(\Delta - \kappa)\tilde{\Psi} = \frac{1}{2}(\mathbf{f} + \epsilon),$$

and the scalar potential $\tilde{\psi}$ as

$$-\Delta\tilde{\psi} = \mathbf{x} \cdot \Delta\tilde{\Psi} + \eta,$$

for some functions ϵ and η. Then,

$$\begin{cases} -(\Delta - \kappa)\tilde{\mathbf{u}}_{\text{part}} + \nabla\tilde{p}_{\text{part}} = \mathbf{f} + \nabla\eta + \epsilon \\ \nabla \cdot \tilde{\mathbf{u}}_{\text{part}} = -\Delta\tilde{\psi} - \mathbf{x} \cdot \Delta\tilde{\Psi} = \eta \end{cases}$$

and in, particular, the divergence error is

$$\|\nabla \cdot \tilde{\mathbf{u}}_{\text{part}}\|_{L^2(\Omega)} = \|\eta\|_{L^2(\Omega)}. \tag{17}$$

Hence:

a) The function $\tilde{\mathbf{u}}_{\text{part}}$ is not divergence free.
b) If $\mathbf{f}$ has low regularity then the error $\|\epsilon\|_{L^2(\Omega)}$ may be high because $\tilde{\Psi}$ is a superposition of smooth functions. However, the term $\mathbf{x} \cdot \Delta\tilde{\Psi}$ is smooth so the error (17) should be small, meaning that we should obtain low divergence error even when $\mathbf{f}$ is nonsmooth.

4 Numerical method based on divergence-free functions

In this section, we use Theorem 1 to construct a set of basis functions for the approximation of the velocity term which satisfy exactly the divergence-free condition.

Recall the set $\mathcal{C} \subset \mathbb{R}$ such that the problem (5) has a unique solution for each $L \in H^1(\Omega)'$ if and only if $\kappa \notin \mathcal{C}$. We will also use the following rule

$$H_0^{(1)'} = -H_1^{(1)}$$

for the derivative of the Hankel function.

4.1 Divergence free basis functions in dimension $d = 2$

Consider a 2D regular stream function ϕ satisfying

$$\Delta\phi + \kappa\phi = 0 \tag{18}$$

in Ω. Then, the vector function

$$\mathbf{u} = \nabla^{\perp}\phi$$

where $\nabla^{\perp}\phi = (-\partial_2\phi, \partial_1\phi)$, satisfies the system

$$\begin{cases} \Delta\mathbf{u} + \kappa\mathbf{u} = 0 & \text{in } \Omega, \\ \nabla \cdot \mathbf{u} = 0 & \text{in } \Omega, \end{cases} \tag{19}$$

For instance, if we take a fundamental solution for the Helmholtz equation,

$$\phi(\mathbf{x}) = \frac{\mathrm{i}}{4}H_0^{(1)}(\sqrt{\kappa}|\mathbf{x}|),$$

then this stream function satisfies (18) in $\mathbb{R}^2 \setminus \{0\}$ and

$$\mathbf{u}(\mathbf{x}) = \nabla^{\perp}\phi(\mathbf{x}) = -\frac{\mathrm{i}}{4}\sqrt{\kappa}\frac{\mathbf{x}^{\perp}}{|\mathbf{x}|}H_1^{(1)}(\sqrt{\kappa}|\mathbf{x}|), \quad \mathbf{x}^{\perp} = (-x_2, x_1), \tag{20}$$

satisfies (19) in $\Omega = \mathbb{R}^2 \setminus \{0\}$. We now show that functions of the type (20) span a dense subspace in the space of divergence-free functions

$$\ker(\nabla\cdot) = \left\{\mathbf{u} \in \mathbf{L}^2(\Omega) : \nabla \cdot \mathbf{u} = 0 \text{ in } \Omega\right\}.$$

Proposition 1 *Let $I =]a, b[\subset \mathbb{R}^+ \setminus \mathcal{C}$. The set*

$$\left\{\kappa\frac{(\mathbf{x}-\mathbf{y})^{\perp}}{|\mathbf{x}-\mathbf{y}|}H_1^{(1)}(\kappa|\mathbf{x}-\mathbf{y}|)|_{\mathbf{x}\in\Omega} : \kappa \in I, \quad \mathbf{y} \in \hat{\Gamma}\right\} \tag{21}$$

where $\hat{\Gamma} = \partial\hat{\Omega}$, with $\hat{\Omega}$ an open set containing $\overline{\Omega}$, spans a dense subspace in $\ker(\nabla\cdot)$.

Proof From (20) and the identity (see, e.g. [9])

$$\ker(\nabla\cdot) = \nabla^{\perp}H^1(\Omega),$$

it is sufficient to recall (see Theorem 1) that the set

$$\left\{H_0^{(1)}(\kappa|\mathbf{x}-\mathbf{y}|)|_{\mathbf{x}\in\Omega} : \kappa \in I =]a, b[, \quad \mathbf{y} \in \hat{\Gamma}\right\} \tag{22}$$

spans a dense subspace in $H^1(\Omega)$. □

4.2 Divergence free basis functions in dimension $d = 3$

When $d = 3$, we can consider the stream function

$$\phi(\mathbf{x}) = \frac{e^{\mathrm{i}\sqrt{\kappa}|\mathbf{x}|}}{4\pi|\mathbf{x}|}, \quad \mathbf{x} \in \mathbb{R}^3 \setminus \{0\},$$

fundamental solution for the three dimensional Helmholtz equation, and define the following vector valued functions

$$\mathbf{u}^{(j)}(\mathbf{x}) = \nabla \times \left(\phi(\mathbf{x})\mathbf{e}_j\right) = \frac{\left(\mathrm{i}\sqrt{\kappa}|\mathbf{x}| - 1\right)e^{\mathrm{i}\sqrt{\kappa}|\mathbf{x}|}}{4\pi|\mathbf{x}|^3}\left(\mathbf{x} \times \mathbf{e}_j\right) \tag{23}$$

with $\{\mathbf{e}_1, \mathbf{e}_2, \mathbf{e}_3\}$ the standard basis for $\mathbb{R}^3$. These functions satisfy

$$\Delta\mathbf{u}^{(j)} + \kappa\mathbf{u}^{(j)} = 0, \ \nabla \cdot \mathbf{u}^{(j)} = 0, \ \text{in } \mathbb{R}^3 \setminus \{0\}.$$

Furthermore, the following density result holds.

Proposition 2 *Let I and $\tilde{\Gamma}$ be as in Proposition 1. The set*

$$\left\{\frac{(\mathrm{i}\kappa|\mathbf{x}-\mathbf{y}| - 1)\,e^{\mathrm{i}\kappa|\mathbf{x}-\mathbf{y}|}}{4\pi|\mathbf{x}-\mathbf{y}|^3}(\mathbf{x}-\mathbf{y}) \times \mathbf{e}_j|_{\mathbf{x}\in\Omega} : \ \kappa \in I, \ j = 1, 2, 3, \ \mathbf{y} \in \hat{\Gamma}\right\}$$

spans a dense subspace in $\ker(\nabla\cdot)$.

Proof From Theorem 1, the set

$$\text{span}\left\{\varphi_\kappa(\mathbf{x}-\mathbf{y})\mathbf{e}_j : \kappa \in I,\ \mathbf{y} \in \hat{\Gamma},\ j=1,2,3\right\}, \quad \varphi_\kappa(\mathbf{x}) = \frac{e^{\mathrm{i}\kappa|\mathbf{x}|}}{4\pi|\mathbf{x}|},$$

is dense in $\mathbf{H}^1(\Omega)$. Then, by (23),

$$\mathcal{U} := \text{span}\left\{\mathbf{u}_\kappa^{(j)}(\mathbf{x}-\mathbf{y}) : \kappa \in I,\ \mathbf{y} \in \hat{\Gamma},\ j=1,2,3\right\}, \quad \mathbf{u}_\kappa^{(j)}(\mathbf{x}) = \nabla \times \left(\varphi_\kappa(\mathbf{x})\mathbf{e}_j\right)$$

is dense in $\ker(\nabla\cdot)$. Since, in 3D, we have (see, e.g. [9]) $\ker(\nabla\cdot) = \nabla \times \mathbf{H}^1(\Omega)$, we conclude that $\mathcal{U}$ is dense in $\nabla \times \mathbf{H}^1(\Omega)$. □

4.3 Numerical method using divergence free basis functions

We consider the divergence free functions (21) for the approximation of the solenoidal part of a two dimensional body force $\mathbf{f} \in \mathbf{L}^2(\Omega)$.

When a potential function $q \in H^1(\Omega)$ such that

$$\Delta q = \nabla \cdot \mathbf{f}, \text{ in } \Omega,$$

is known, then $\mathbf{f} + \nabla q \in \ker(\nabla\cdot)$ and, using Proposition 1, we can consider an approximation

$$\mathbf{f}(\mathbf{x}) - \nabla q(\mathbf{x}) \approx \sum_{n=1}^{O}\sum_{k=1}^{P} \alpha^{(n,k)}\lambda_n \frac{(\mathbf{x}-\mathbf{y}^{(k)})^\perp}{|\mathbf{x}-\mathbf{y}^{(k)}|} H_1^{(1)}(\lambda_n|\mathbf{x}-\mathbf{y}^{(k)}|), \quad \mathbf{y}^{(k)} \in \hat{\Gamma}, \tag{24}$$

with the corresponding approximation for the particular solution $(\tilde{\mathbf{u}}_{\text{part}}, \tilde{p}_{\text{part}})$ given by

$$\begin{aligned} \tilde{\mathbf{u}}_{\text{part}}(\mathbf{x}) &= \sum_{n=1}^{O}\sum_{k=1}^{P} \frac{\alpha^{(n,k)}}{\lambda_n^2+\kappa}\lambda_n \frac{(\mathbf{x}-\mathbf{y}^{(k)})^\perp}{|\mathbf{x}-\mathbf{y}^{(k)}|} H_1^{(1)}(\lambda_n|\mathbf{x}-\mathbf{y}^{(k)}|) \\ \tilde{p}_{\text{part}} &= q. \end{aligned} \tag{25}$$

For a more general function, some extra basis functions must be added in order to approximate the conservative part of the source.

Based on the density result of Lemma 1, the pressure p_{part} will be approximated by

$$\tilde{p}_{\text{part}}(\mathbf{x}) = -\mathrm{i}\sum_{l=1}^{Q}\sum_{m=1}^{T} \frac{\beta^{(l,m)}}{\mu_l} e^{\mathrm{i}\mu_l \mathbf{x}\cdot\mathbf{d}^{(m)}}. \tag{26}$$

The unknown coefficients $\alpha^{(n,k)}$, $\beta^{(l,m)}$ in (25) and (26) are computed by imposing collocation conditions

$$\begin{aligned} \tilde{\mathbf{f}}(\mathbf{x}^{(j)}) &= -(\Delta-\kappa)\tilde{\mathbf{u}}_{\text{part}}(\mathbf{x}^{(j)}) + \nabla\tilde{p}_{\text{part}}(\mathbf{x}^{(j)}) \\ &= \sum_{n=1}^{O}\sum_{k=1}^{P} \alpha^{(j,k)}\lambda_n \frac{(\mathbf{x}^{(j)}-\mathbf{y}^{(k)})^\perp}{|\mathbf{x}^{(j)}-\mathbf{y}^{(k)}|} H_1^{(1)}(\lambda_n|\mathbf{x}^{(j)}-\mathbf{y}^{(k)}|) \\ &\quad + \sum_{l=1}^{Q}\sum_{m=1}^{T} \beta^{(l,m)}\mathbf{d}^{(m)} e^{\mathrm{i}\mu_l \mathbf{x}^{(j)}\cdot\mathbf{d}^{(m)}} \\ &= \mathbf{f}(\mathbf{x}^{(j)}), \quad \mathbf{x}^{(j)} \in \Omega. \end{aligned} \tag{27}$$

In order to give a matrix formulation for the computation of the coefficients of the approximation $(\tilde{\mathbf{u}}_{\text{part}}, \tilde{p}_{\text{part}})$, we define the matrices

$$D = \begin{bmatrix} \lambda_1 \frac{-(x_2^{(1)}-y_2^{(1)})}{|\mathbf{x}^{(1)}-\mathbf{y}^{(1)}|} H_1^{(1)}(\lambda_1|\mathbf{x}^{(1)}-\mathbf{y}^{(1)}|) & \dots & \lambda_O \frac{-(x_2^{(1)}-y_2^{(P)})}{|\mathbf{x}^{(1)}-\mathbf{y}^{(P)}|} H_1^{(1)}(\lambda_O|\mathbf{x}^{(1)}-\mathbf{y}^{(P)}|) \\ \vdots & \ddots & \vdots \\ \lambda_1 \frac{-(x_2^{(K)}-y_2^{(1)})}{|\mathbf{x}^{(K)}-\mathbf{y}^{(1)}|} H_1^{(1)}(\lambda_1|\mathbf{x}^{(K)}-\mathbf{y}^{(1)}|) & \dots & \lambda_O \frac{-(x_2^{(K)}-y_2^{(P)})}{|\mathbf{x}^{(K)}-\mathbf{y}^{(P)}|} H_1^{(1)}(\lambda_O|\mathbf{x}^{(K)}-\mathbf{y}^{(P)}|) \\ \lambda_1 \frac{(x_1^{(1)}-y_1^{(1)})}{|\mathbf{x}^{(1)}-\mathbf{y}^{(1)}|} H_1^{(1)}(\lambda_1|\mathbf{x}^{(1)}-\mathbf{y}^{(1)}|) & \dots & \lambda_O \frac{(x_1^{(1)}-y_1^{(P)})}{|\mathbf{x}^{(1)}-\mathbf{y}^{(P)}|} H_1^{(1)}(\lambda_O|\mathbf{x}^{(1)}-\mathbf{y}^{(P)}|) \\ \vdots & \ddots & \vdots \\ \lambda_1 \frac{(x_1^{(K)}-y_1^{(1)})}{|\mathbf{x}^{(K)}-\mathbf{y}^{(1)}|} H_1^{(1)}(\lambda_1|\mathbf{x}^{(K)}-\mathbf{y}^{(1)}|) & \dots & \lambda_O \frac{(x_1^{(K)}-y_1^{(P)})}{|\mathbf{x}^{(K)}-\mathbf{y}^{(P)}|} H_1^{(1)}(\lambda_O|\mathbf{x}^{(K)}-\mathbf{y}^{(P)}|) \end{bmatrix}_{2K\times(Ox\times P)},$$

$$E = \begin{bmatrix} d_1^{(1)} e^{\mathrm{i}\mu_1 \mathbf{x}^{(1)}\cdot\mathbf{d}^{(1)}} & \dots & d_1^{(T)} e^{\mathrm{i}\mu_Q \mathbf{x}^{(1)}\cdot\mathbf{d}^{(T)}} \\ \vdots & \ddots & \vdots \\ d_1^{(1)} e^{\mathrm{i}\mu_1 \mathbf{x}^{(K)}\cdot\mathbf{d}^{(1)}} & \dots & d_1^{(T)} e^{\mathrm{i}\mu_Q \mathbf{x}^{(K)}\cdot\mathbf{d}^{(T)}} \\ d_2^{(1)} e^{\mathrm{i}\mu_1 \mathbf{x}^{(1)}\cdot\mathbf{d}^{(1)}} & \dots & d_2^{(T)} e^{\mathrm{i}\mu_Q \mathbf{x}^{(1)}\cdot\mathbf{d}^{(T)}} \\ \vdots & \ddots & \vdots \\ d_2^{(1)} e^{\mathrm{i}\mu_1 \mathbf{x}^{(K)}\cdot\mathbf{d}^{(1)}} & \dots & d_2^{(T)} e^{\mathrm{i}\mu_Q \mathbf{x}^{(K)}\cdot\mathbf{d}^{(T)}} \end{bmatrix}_{2K\times(Q\times T)},$$

$$X = \begin{bmatrix} \alpha^{(j,k)} \\ \beta^{(l,m)} \end{bmatrix}_{(O\times P+Q\times T)\times 1}, \qquad G = \begin{bmatrix} f_1(\mathbf{x}^{(1)}) \\ \vdots \\ f_1(\mathbf{x}^{(K)}) \\ f_2(\mathbf{x}^{(1)}) \\ \vdots \\ f_2(\mathbf{x}^{(K)}) \end{bmatrix}_{2K\times 1},$$

and the corresponding linear system, which imposes $\tilde{\mathbf{f}}(\mathbf{x}^{(j)}) = \mathbf{f}(\mathbf{x}^{(j)})$, $j = 1, ..., K$, namely, the last identity in (27), is

$$[D|E]_{2K\times(O\times P+Q\times T)}\, X = G. \tag{28}$$

5 The method of fundamental solutions for Stokes and Brinkman systems

In this section, we recall the MFS for solving Stokes and Brinkman systems with body force $\mathbf{f} = \mathbf{0}$ and Dirichlet boundary conditions.

The fundamental solution of the modified Helmholtz's equation,

$$-\Delta E_\kappa + \kappa E_\kappa = \delta, \text{ in } \mathbb{R}^d, \qquad (\kappa > 0)$$

can be written in terms of the modified Bessel functions of the second kind (see [8])

$$E_\kappa(\mathbf{x}) = \frac{1}{2\pi}\left(\frac{\sqrt{\kappa}}{2\pi|\mathbf{x}|}\right)^{d/2-1} K_{d/2-1}(\sqrt{\kappa}|\mathbf{x}|). \tag{29}$$

where the relation

$$K_\alpha(z) = \frac{\pi \mathrm{i}^{\alpha+1}}{2} H_\alpha^{(1)}(\mathrm{i}z)$$

can be used if $z \in \mathbb{R}$. When $d = 2$ and $d = 3$, (29) takes the form

$$E_\kappa(\mathbf{x}) = \begin{cases} \dfrac{K_0(\sqrt{\kappa}|\mathbf{x}|)}{2\pi} = \dfrac{\mathrm{i}}{4} H_0^{(1)}(\mathrm{i}\sqrt{\kappa}|\mathbf{x}|), & \text{when } d = 2 \\ \dfrac{\exp(-\sqrt{\kappa}|\mathbf{x}|)}{4\pi|\mathbf{x}|}, & \text{when } d = 3. \end{cases}$$

We now apply the method of fundamental solutions for solving the homogeneous problem (3). A fundamental solution $(\mathbf{U}_\kappa, \mathbf{P}_\kappa)$ for the Brinkman system satisfies

$$\begin{cases} -(\Delta - \kappa)\mathbf{U}_\kappa + \nabla \mathbf{P}_\kappa = \delta \mathbf{I} & \text{in } \Omega \\ \nabla \cdot \mathbf{U}_\kappa = 0 & \text{in } \Omega \end{cases}$$

or, for each $j = 1, ..., d$,

$$\begin{cases} -(\Delta - \kappa)(\mathbf{U}_\kappa \mathbf{e}_j) + \nabla(\mathbf{P}_\kappa \cdot \mathbf{e}_j) = \delta \mathbf{e}_j & \text{in } \Omega \\ \nabla \cdot (\mathbf{U}_\kappa \mathbf{e}_j) = 0 & \text{in } \Omega \end{cases}$$

where $\{\mathbf{e}_1, \ldots, \mathbf{e}_d\}$ is the standard basis in $\mathbb{R}^d$ and δ the Dirac delta function. When $\kappa = 0$, we recover the Stokes problem and the fundamental solution is given by a tensor velocity component

$$\mathbf{U}_0(\mathbf{x}) = \begin{cases} \dfrac{1}{4\pi}\left(-\mathbf{I}\log|\mathbf{x}| + \dfrac{\mathbf{x}\otimes\mathbf{x}}{|\mathbf{x}|^2}\right), & \text{when } d = 2 \\ \dfrac{1}{8\pi}\left(\mathbf{I}\dfrac{1}{|\mathbf{x}|} + \dfrac{\mathbf{x}\otimes\mathbf{x}}{|\mathbf{x}|^3}\right), & \text{when } d = 3 \end{cases}$$

(here, $\otimes$ stands for the dyadic product) and a pressure vector

$$\mathbf{P}_0(\mathbf{x}) = \mathbf{P}(\mathbf{x}) = \frac{1}{2(d-1)\pi}\frac{\mathbf{x}}{|\mathbf{x}|^d}, \quad d = 2, 3.$$

When $\kappa > 0$, the pressure is the same as above, $\mathbf{P}_k(\mathbf{x}) = \mathbf{P}(\mathbf{x})$, but the Brinkman velocity tensor is (see, e.g. [26])

$$\mathbf{U}_\kappa(\mathbf{x}) = \begin{cases} \dfrac{K_0(\sqrt{\kappa}|\mathbf{x}|)}{2\pi}\left(\mathbf{I} - \dfrac{\mathbf{x}\otimes\mathbf{x}}{|\mathbf{x}|^2}\right) + \dfrac{K_1(\sqrt{\kappa}|\mathbf{x}|) - \frac{1}{\sqrt{k}|\mathbf{x}|}}{2\pi\sqrt{\kappa}|\mathbf{x}|}\left(\mathbf{I} - 2\dfrac{\mathbf{x}\otimes\mathbf{x}}{|\mathbf{x}|^2}\right), & \text{when } d = 2, \\ \dfrac{e^{-\sqrt{\kappa}|\mathbf{x}|}}{4\pi|\mathbf{x}|}\left(\mathbf{I} - \dfrac{\mathbf{x}\otimes\mathbf{x}}{|\mathbf{x}|^2}\right) + \dfrac{(1+\sqrt{\kappa}|\mathbf{x}|)e^{-\sqrt{\kappa}|\mathbf{x}|} - 1}{4\pi\kappa|\mathbf{x}|^3}\left(\mathbf{I} - 3\dfrac{\mathbf{x}\otimes\mathbf{x}}{|\mathbf{x}|^2}\right), & \text{when } d = 3. \end{cases}$$

The following result concerning density of Stokeslets functions is well known (see [3] for the case $\kappa = 0$ and [14] for $\kappa > 0$) and justifies the approximation of boundary velocities in $\mathbf{H}_{\mathbf{n}}^{\frac{1}{2}}(\Gamma)$ using the method of fundamental solutions.

Proposition 3 *Let $\hat{\Omega}$ be an open, simply connected domain containing $\overline{\Omega}$ with regular boundary $\hat{\Gamma} = \partial\hat{\Omega}$. The set*

$$\left\{ \mathbf{U}_\kappa(\mathbf{x}-\mathbf{y})\mathbf{e}_j|_{\mathbf{x}\in\Gamma} : \mathbf{y} \in \hat{\Gamma},\ j = 1, \ldots, d \right\} \tag{30}$$

spans a dense subspace in $\mathbf{H}_{\mathbf{n}}^{\frac{1}{2}}(\Gamma)$ when $\kappa \geq 0$ and $d = 3$. The same result holds for the two dimensional Brinkman tensor ($\kappa > 0$) whilst for the two dimensional Stokes tensor we must add constants $\mathbf{c} \in \mathbb{R}^2$ to the set (30).

The solution of the homogeneous problem is approximated by a superposition of fundamental solutions,

$$\mathbf{u}_{\text{hom}}(\mathbf{x}) \approx \tilde{\mathbf{u}}_{\text{hom}}(\mathbf{x}) = \sum_{j=1}^{d}\sum_{k=1}^{N} \gamma^{(j,k)}\mathbf{U}(\mathbf{x}-\mathbf{y}^{(k)})\mathbf{e}_j,$$

$$p_{\text{hom}}(\mathbf{x}) \approx \tilde{p}_{\text{hom}}(\mathbf{x}) = \sum_{j=1}^{d}\sum_{k=1}^{N} \gamma^{(j,k)}P_j(\mathbf{x}-\mathbf{y}^{(k)}),$$

where $P_j = \mathbf{P}\cdot\mathbf{e}_j$, $\mathbf{y}^{(1)}, \ldots, \mathbf{y}^{(N)} \in \hat{\Gamma}$ are source points and the coefficients $\gamma^{(j,k)}$ are computed by imposing the boundary condition

$$\tilde{\mathbf{u}}_{\text{hom}}(\mathbf{x}_l) = \mathbf{g}(\mathbf{x}^{(l)}) - \tilde{\mathbf{u}}_{\text{part}}(\mathbf{x}^{(l)})$$

on some boundary collocation points $\mathbf{x}^{(1)}, \ldots, \mathbf{x}^{(M)} \in \Gamma$.

6 Numerical experiments

We present three numerical examples in order to illustrate the proposed methods for 2D Brinkman problems.

Example 1 Let $\Omega = B(0,1) = \left\{\mathbf{x} = (x_1, x_2) \in \mathbb{R}^2 : |\mathbf{x}| < 1\right\}$ and consider the body force

$$\begin{aligned}\mathbf{f}(\mathbf{x}) \ = \ & \left(2x_1 - e^{-x_1^2+\cos(x_2)}\sin(x_2)(-4+4x_1^2-3\cos(x_2)+\sin(x_2)^2)\right)\mathbf{e}_1 \\ & -\left(1+e^{-x_1^2+\cos(x_2)}x_1(13-8x_1^2+2\cos(x_2)+\cos(2x_2))\right)\mathbf{e}_2,\end{aligned} \tag{31}$$

with $\{\mathbf{e}_1, \mathbf{e}_2\}$ the standard basis of $\mathbb{R}^2$. Consider the boundary data

$$\mathbf{g}(\mathbf{x}) = \sin(x_2)e^{-x_1^2+\cos(x_2)}\mathbf{e}_1 - 2x_1e^{-x_1^2+\cos(x_2)}\mathbf{e}_2$$

and let $\kappa = 1$. The solution for the corresponding Brinkman system is

$$\mathbf{u}(\mathbf{x}) = \sin(x_2)e^{-x_1^2+\cos(x_2)}\mathbf{e}_1 - 2x_1e^{-x_1^2+\cos(x_2)}\mathbf{e}_2, \quad p(\mathbf{x}) = x_1^2 - x_2 + c.$$

We consider the Neuber-Papkovich approximation for the body force with directions

$$S = \left\{\left(\cos\left(\frac{\pi}{31}j\right), \sin\left(\frac{\pi}{31}j\right)\right),\ j = 0, \ldots, 61\right\}$$

and frequencies

$$\Sigma = \{0.9 \times j,\ j = 1, \ldots, 15\},$$

meaning $M \times N = 945$ sources. In order to avoid oscillations near the boundary for the approximation of the body force, we considered collocation in the larger domain $\tilde{\Omega} = B(0, 1.5)$. Here, 945 collocation points were selected from points $\mathbf{x}^{(j)}$ on an uniform mesh in $[-1.5, 1.5]^2$ such that $\mathbf{x}^{(j)} \in B(0, 1.5)$.

For solving the homogeneous problem with the MFS, we considered 315 collocation points on the boundary $\Gamma = \partial B(0, 1)$ and the same amount of source points on the artificial boundary $\hat{\Gamma} = \partial B(0, 1.1)$. In Fig. 1 we plot the absolute error $|u_1 - \tilde{u}_1|$ (on the left) and $|u_2 - \tilde{u}_2|$ (on the right). In Fig. 2 we plot the absolute error for the pressure.

Note that the body force $\mathbf{f}$ defined in (31) satisfies

$$\nabla \cdot \mathbf{f} = 2 \text{ in } \Omega.$$

Hence, in order to apply the second method for this problem we can consider

$$\tilde{p}_{\text{part}}(\mathbf{x}) = x_1^2$$

because this function satisfies $\Delta \tilde{p}_{\text{part}} = \nabla \cdot \mathbf{f}$. The respective particular velocity is given by (25) with coefficients such that (24) is enforced on the same 945 domain collocations points $\mathbf{x}^{(j)} \in B(0, 1.5)$. The source points were

$$\mathbf{y}^{(k)} \in \{1.8\,(\cos(0.04\,j), \sin(0.04\,j)),\ j = 0, \ldots, 157\}$$

and the frequencies

$$\lambda_n \in \{0.02 + 0.9\,j,\ j = 0, \ldots, 38\}.$$

For the homogeneous problem we used the same collocation and source points of the previous method. In Figs. 3 and 4, we present the absolute errors for each coordinate of the velocity and the pressure. As we can see, the approximation obtained with this method is also in good agreement with the solution, although with slightly worst errors and some small oscillations near the boundary. In order to investigate this

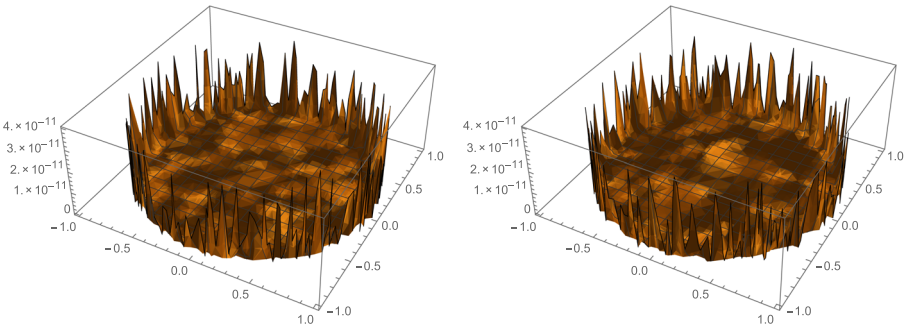

Fig. 1 Absolute errors for the coordinates of the velocity (Example 1)

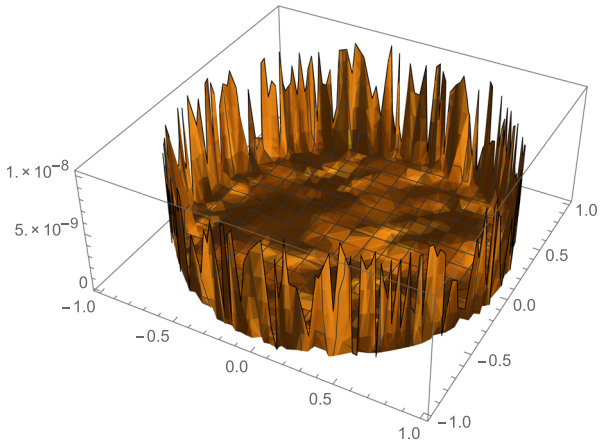

Fig. 2 Same as above but for the pressure (Example 1)

behaviour we computed relative errors in $B(0,1)\setminus B(0,0.7)$ using L^2 and H^1 norms, with values

$$\frac{||\mathbf{u}-\tilde{\mathbf{u}}||_{\mathbf{L}^2}}{||\mathbf{u}||_{\mathbf{L}^2}} \approx 10^{-10}, \quad \frac{||\mathbf{u}-\tilde{\mathbf{u}}||_{\mathbf{H}^1}}{||\mathbf{u}||_{\mathbf{H}^1}} \approx 8\times 10^{-9}$$

for the velocity and

$$\frac{||p-\tilde{p}||_{L^2}}{||p||_{L^2}} \approx 3\times 10^{-8}$$

for the pressure.

Example 2 In this example, we present some numerical tests in order to study the influence of the frequencies on the approximation of the particular solution. We consider the same domain $\Omega = B(0,1)$ and the body force

$$\mathbf{f}(\mathbf{x}) = -\exp\left(-\frac{11}{2}|\mathbf{x}|^2\right)\mathbf{e}_1 - \cosh(x_1^2 - x_2^2)\mathbf{e}_2. \tag{32}$$

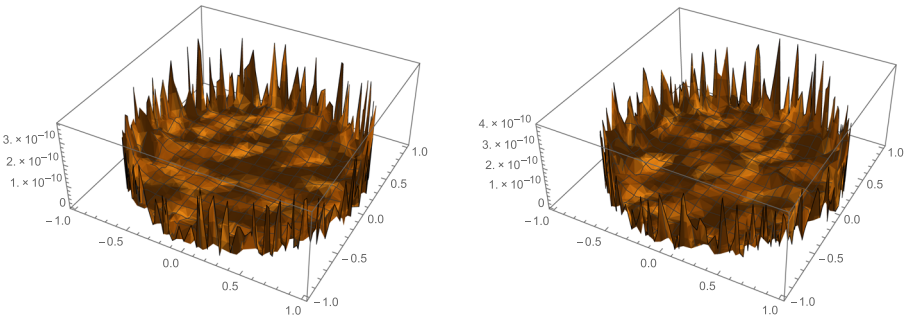

Fig. 3 Absolute error for the velocity field applying method 2. Left—first coordinate. Right—second coordinate (Example 1)

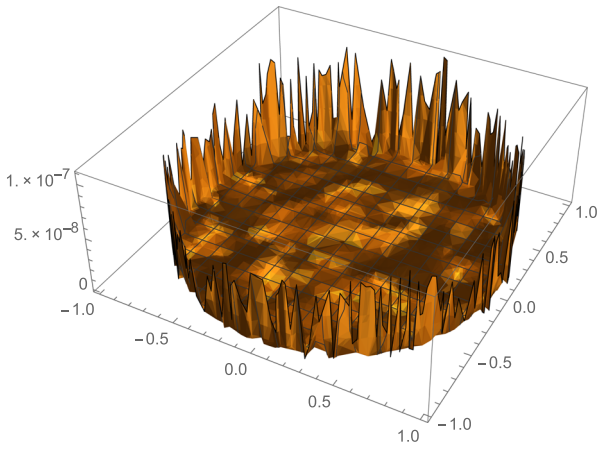

Fig. 4 Same as in the previous figure but for the pressure

Define the RMS error for the force approximation with $J = 2000$

$$\mathrm{RMS}_{\mathbf{f}} = \sqrt{\frac{\sum_{j=1}^{J} |f_1(\mathbf{z}^{(j)}) - \tilde{f}_1(\mathbf{z}^{(j)})|^2 + |f_2(\mathbf{z}^{(j)}) - \tilde{f}_2(\mathbf{z}^{(j)})|^2}{4000}}$$

at J randomly generated points $\mathbf{z}^{(j)} \in \overline{\Omega}$ and also

$$\mathrm{RMS}_{div} = \sqrt{\frac{\sum_{j=1}^{J} |\partial_1 \tilde{u}_1(\mathbf{z}^{(j)}) + \partial_2 \tilde{u}_2(\mathbf{z}^{(j)})|^2}{2000}}$$

for the divergence error.

We start by computing the above errors as function of $\kappa \in \{0, 1, 5, 10\}$ for the Neuber-Papkovich method. We obtained similar error values for these frequencies κ (see Table 1). Furthermore, the divergence error (column 4 of the same table) is smaller than the $\mathrm{RMS}_{\mathbf{f}}$ error and thus consistent with Remark 1.

Next tests concerns the computation of the L^2 errors and condition numbers as a function of the number of basis functions. We considered $\kappa = 0$ and 50 equally distributed directions on $\partial B(0, 1)$ with frequencies λ_n belonging to

$$\Sigma_s = \{0.1 + j,\ \ j = 0, \ldots, s\}\,.$$

Table 1 RMS and maximum errors as function of κ. Domain collocation points, frequencies and directions were borrowed from the previous example

	$\mathrm{RMS}_{\mathbf{f}}$	$\|\tilde{\mathbf{f}} - \mathbf{f}\|_\infty$	RMS_{div}	$\|\nabla \cdot \tilde{\mathbf{u}}_{\mathrm{par}}\|_\infty$
$\kappa = 0$	1.6×10^{-9}	2.0×10^{-8}	8.4×10^{-11}	8.0×10^{-10}
$\kappa = 1$	1.4×10^{-9}	1.5×10^{-8}	7.6×10^{-11}	8×10^{-10}
$\kappa = 5$	1.2×10^{-9}	1.5×10^{-8}	6.7×10^{-11}	7.2×10^{-10}
$\kappa = 10$	1.2×10^{-9}	$1. \times 10^{-8}$	6.1×10^{-11}	6.5×10^{-10}

Therefore, the number of plane waves basis functions is $(s+1)\times 50$. In order to obtain square systems, we considered $(s+1)\times 50$ uniformly distributed collocation points in $B(0,1.5)$. The corresponding results are presented in Table 2.

We can have large condition numbers for the system and yet good error results. This is a common feature of some meshless methods and is an example of the so called Schaback's uncertainty principle (cf. [22]). Better conditioned systems can be obtained by using, for instance, the Tikhonov regularization method. This can be seen in Table 3 where we applied regularization to (16) using frequencies in Σ_{29}, meaning that we solved (recall (16))

$$(\alpha I + A^* A)X_i = A^* B_i, \quad (\alpha I + A^* A)Y = A^* C \tag{33}$$

where $\alpha > 0$ is the regularization parameter and A^* denotes the conjugate transpose. For each parameter, the total computational time for the 1500×1500 systems (33) was 70s.

Next tests concerns the computation of the L^2 error and condition number using the second method. Note that, for the body force (32), it is not clear how to obtain a potential function satisfying $\Delta q = \nabla\cdot\mathbf{f}$. Hence, we consider the expansions (25) for $\tilde{\mathbf{u}}_{\text{part}}$ and (26) for $\tilde{p}_{\text{part}}$. Source points $\mathbf{y}^{(k)}$ for the velocity were 50 equally distributed points on $\hat{\Gamma} = \partial B(0,1.8)$ with frequencies λ_n belonging to

$$\Sigma_s = \{0.1 + j,\ \ j = 0,\ldots,s\}$$

for several values of s and thus the number of solenoidal basis functions is $(s+1)\times 50$. For the plane wave basis functions in (26), 50 directions were considered, with frequencies $\mu_l \in \Sigma_s$. In order to obtain square systems, we considered $(s+1)\times 50$ uniformly distributed collocation points in $B(0,1.5)$. The corresponding error results are presented in Table 4.

Total computation time for the 1500×1500 system $(D|E)X = G$ with set of frequencies Σ_{14} was 100s. Again, we obtained low error values but with high condition numbers. Furthermore, note that the Neuber–Papkovich approximations lead to linear systems for scalar potentials whilst using divergence free functions we are solving vector valued equations. Thus, when using Neuber-Papkovich with frequencies in Σ_{29} the linear system with the same order in method 2 is for frequencies in Σ_{14}. Comparing the corresponding results from Tables 2 and 4, we see better results for both error and conditioning using the first method. However, for the same set of frequencies, method 2 gives better results.

Table 2 L^2 error and condition number as function of the number of basis functions using the Neuber–Papkovich potentials

Set of frequencies	$\|\mathbf{f}-\tilde{\mathbf{f}}\|_{L^2}$	$cond_2(A)$
Σ_9	5.6×10^{-2}	1.6×10^{19}
Σ_{14}	4.2×10^{-6}	1.4×10^{19}
Σ_{19}	1.4×10^{-7}	2.2×10^{19}
Σ_{24}	1.2×10^{-7}	3.2×10^{19}
Σ_{29}	2.3×10^{-7}	5.3×10^{19}

Table 3 $\mathbf{L}^2$ error and condition number as function of the regularization parameter

Regularization parameter	$\|\|\mathbf{f}-\tilde{\mathbf{f}}\|\|_{\mathbf{L}^2}$	$cond_2(\alpha I + A^*A)$
10^{-9}	1.4×10^{-5}	1.1×10^{14}
10^{-10}	4.1×10^{-6}	1.2×10^{15}
10^{-11}	1.9×10^{-6}	9.4×10^{16}
10^{-12}	2.8×10^{-5}	2.2×10^{19}
10^{-13}	1.8×10^{-5}	2.3×10^{19}

Table 4 L^2 error and condition number as function of the number of basis functions

Set of frequencies	$\|\|\mathbf{f}-\tilde{\mathbf{f}}\|\|_{L^2}$	$cond_2(D\|E)$
Σ_9	0.7×10^{-4}	5.0×10^{20}
Σ_{14}	9.7×10^{-6}	1.7×10^{21}
Σ_{19}	5.9×10^{-10}	1.2×10^{21}
Σ_{24}	3.5×10^{-10}	1.2×10^{21}
Σ_{29}	2.04×10^{-9}	4.1×10^{21}

Table 5 L^2 error for the approximation of a conservative body force

Set of frequencies	$\|\|\mathbf{f}-\tilde{\mathbf{f}}\|\|_{L^2}$
Σ_9	1.3×10^{-7}
Σ_{14}	8.6×10^{-8}
Σ_{19}	1.3×10^{-8}

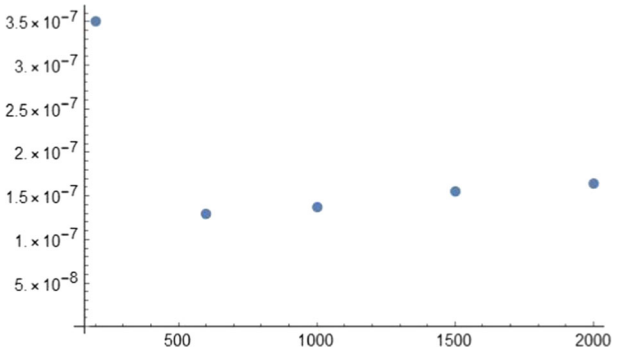

Fig. 5 L^2 error as function of the number of collocation points. Set of source frequencies was Σ_9

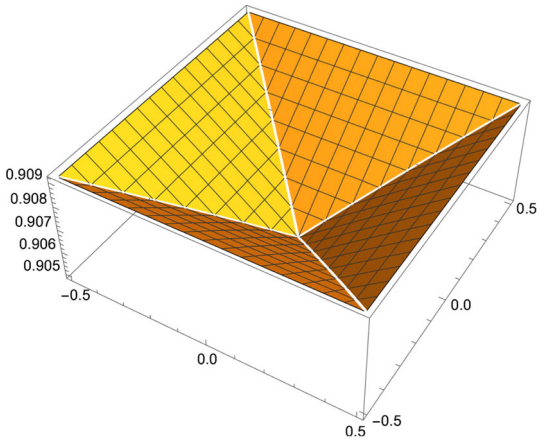

Fig. 6 First coordinate of the body force (Example 3)

When the source is conservative, we can take $\tilde{\mathbf{u}}_{part} = \mathbf{0}$ and use only (26) for the approximation of $\mathbf{f}$. For instance, if

$$\begin{aligned}\mathbf{f}(\mathbf{x}) &= -\exp(x_1x_2)x_2\sin(5x_2)\mathbf{e}_1 - (5\cos(5x_2) + x_1\sin(5x_2))\exp(x_1x_2)\mathbf{e}_2\\ &= -\nabla(\exp(x_1x_2)\sin(5x_2))\end{aligned}$$

then, using the same scheme for collocation and source points, we obtained the results presented in Table 5.

Changing the number of collocation points did not decreased the L^2 error. For instance, considering nested sets of collocation points and Σ_9 as the set of source frequencies error was of the order 10^{-7} except when considering 100 collocation points. In this case the error was 6.3×10^{-4}. Error results for 200, 600, 1000, 1500 and 2000 collocation points are presented in Fig. 5.

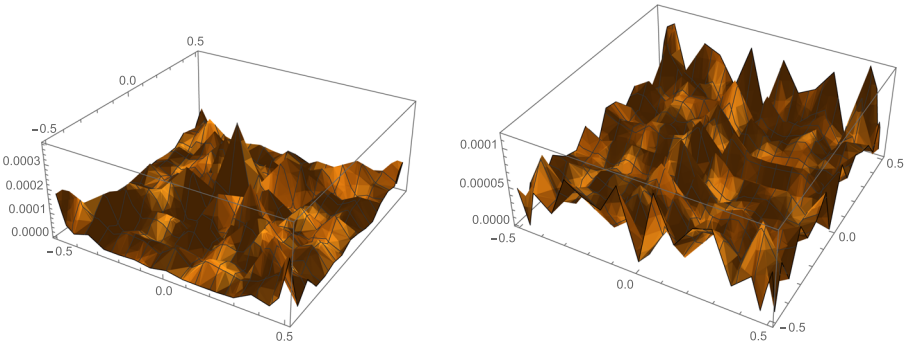

Fig. 7 Absolute error for the approximation of the body force using the Neuber potentials. On the left, for the first coordinate. On the right, for the second coordinate

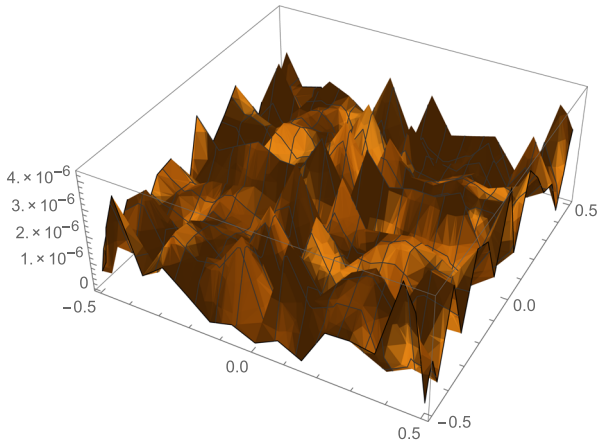

Fig. 8 Absolute error for the divergence

Example 3 For this last example, a square domain $\Omega =]-0.5, 0.5[^2$ was considered and the force term was ($|\mathbf{x}|_\infty$ stands for the maximum vector norm)

$$\mathbf{f}(\mathbf{x}) = \exp\left(-\frac{1}{10 + |\mathbf{x}|_\infty}\right)\mathbf{e}_1 - \log(1 + |\mathbf{x}|^2)\mathbf{e}_2$$

(see Fig. 6 for a picture of the nonsmooth coordinate function f_1) with $\kappa = 5$. On the boundary, $\Gamma = \partial\Omega$, the null condition $\mathbf{u}|_\Gamma = \mathbf{0}$ was considered.

Regarding the Neuber-Papkovich method, we considered 1200 source points and the same amount of collocation points, placed on an uniform grid in the larger domain $B(0, 1)$. For the homogeneous problem we considered 400 collocation points and the same amount of points on the artificial boundary $\hat{\Gamma} = \partial B(0, 1)$.

Figure 7 shows plots for the componentwise body force error. Here, we obtained the RMS error 5.6×10^{-5}. In Fig. 8 we show the absolute error for the divergence. The corresponding RMS error was 1.9×10^{-6}.

On the boundary we obtained the RMS error 1.2×10^{-5} and in Fig. 9 we show the componentwise absolute boundary error on the right side wall of the boundary, $\{0.5\} \times [-0.5, 0.5]$.

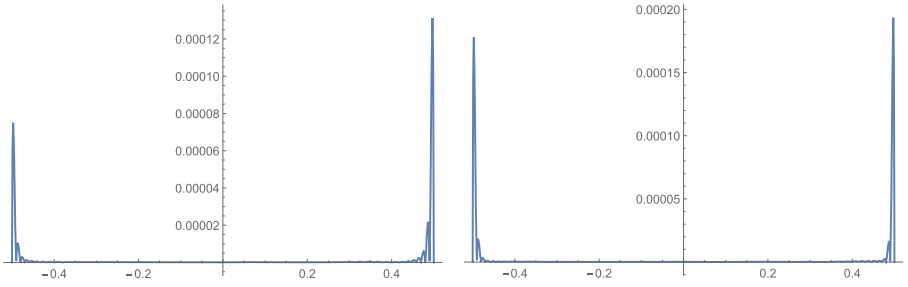

Fig. 9 Absolute boundary error on $\{0.5\} \times [-0.5, 0.5]$. Same as above for the first and second coordinates

For the divergence-free method we considered the same scheme for the homogeneous problem and used the same domain points for the particular solution approximation. Overall the results were similar to the Neuber-Papkovich method with $\mathrm{RMS}_{\mathbf{f}} \approx 3.1 \times 10^{-5}$ and maximum absolute errors 3×10^{-4} and 6×10^{-5} for the first and second coordinate approximation, respectively.

7 Conclusions

Two meshless methods for the numerical approximation of nonhomogeneous Stokes and Brinkman systems in two- and three- dimensional domains were presented. The first method is based on a new class of Neuber-Papkovich potentials representation for the particular solution. The second method relies on a new construction of divergence-free basis functions, based on a Helmholtz decomposition. Particular solutions for such constructions in two- and three-dimensional problems were provided and density results were established. These density results prove that the approximation of the force term is feasible using these basis functions. Numerical simulations illustrate the good performance of both developed methods.

Funding C. J. S. Alves and A. L. Silvestre acknowledge the financial support of the Portuguese FCT - Fundação para a Ciência e a Tecnologia, through the projects UIDB/04621/2020 and UIDP/04621/2020 of CEMAT/IST-ID.

Declarations

Conflict of interest The authors declare no competing interests.

References

1. Abramowitz, M., Stegun, I.: Handbook of Mathematical Functions with Formulas, Graphs, and Mathematical Tables. Dover, New York (1964)
2. Alves, C.J.S., Chen, C.S.: A new method of fundamental solutions applied to nonhomogeneous elliptic problems. Adv. Comput. Math. **23**, 125–142 (2005)
3. Alves, C.J.S., Silvestre, A.L.: Density results using Stokeslets and a method of fundamental solutions for the Stokes equations. Eng. Anal. Bound. Elem. **28**, 1245–1252 (2004)
4. Barnett, A.H., Betcke, T.: Stability and convergence of the method of fundamental solutions for Helmholtz problems on analytic domains. J. Comput. Phys. **227**(14), 7003–7026 (2008)
5. Bogomolny, A.: Fundamental solutions method for elliptic boundary value problems. SIAM J. Numer. Anal. **22**, 644–669 (1985)
6. Brinkman, H.C.: A calculation of the viscous force exerted by a flowing fluid in a dense swarm of particles. Appl. Sci. Res. **A1**, 27–34 (1949)
7. Cheng, A.H.D., Hong, Y.: An overview of the method of fundamental solutions - solvability, uniqueness, convergence, and stability. Eng. Anal. Bound. Elem. **120**, 118–152 (2020)
8. Evans, L.: Partial differential equations Graduate Studies in Mathematics, vol. 19. American Mathematical Society, Providence (1998)
9. Girault, V., Raviart, P.-A.: Finite element methods for Navier-Stokes equations. Theory and algorithms. In: Springer Series in Computational Mathematics, vol. 5. Springer, Berlin (1986)
10. Katsurada, M., Okamoto, H.: A mathematical study of the charge simulation method I. J. Fac. Sci. Univ. Tokyo Sect. IA Math. **35**, 507–518 (1988)

11. Karageorghis, A., Lesnic, D.: The method of fundamental solutions for the Oseen steady-state viscous flow past obstacles of known or unknown shapes. Numer. Methods Partial Differ. Equ. **35**(6), 2103–2119 (2019)
12. Krotkiewski, M., Ligaarden, I.S., Lie, K.-A., Schmid, D.W.: On the importance of the Stokes-Brinkman equations for computing effective permeability in carbonate karst reservoirs. Commun. Comput. Phys. **10**(5), 1315–1332 (2011)
13. Li, X.: On convergence of the method of fundamental solutions for solving the Dirichlet problem of Poisson's equation. Adv. Comp. Math **23**, 265–277 (2005)
14. Martins, N.F.M., Rebelo, M.: Meshfree methods for nonhomogeneous Brinkman flows. Comput. Math. with Appl. **68**(8), 872–886 (2014)
15. McLean, W.: Strongly Elliptic Systems and Boundary Integral Equations. Cambridge University Press, New-York (2000)
16. Nath, D., Kalra, M.S., Munshi, P.: One-stage method of fundamental and particular solutions (MFS-MPS) for the steady Navier-Stokes equations in a lid-driven cavity. Eng. Anal. Bound. Elem. **58**, 39–47 (2015)
17. Neuber, H.: Ein neuer Ansatz zur lösung räumlicher Probleme der elastizitätstheorie. Der Hohlkegel unter Einzellast als Beispiel. Z. Angew. Math. Mech. **14**, 203–212 (1934)
18. Nguyen, V.P., Rabczuk, T., Bordas, S., Duflot, M.: Meshless methods: a review and computer implementation aspects. Math. Comput. Simul. **79**(3), 763–813 (2008)
19. Ogata, H., Katsurada, M.: Convergence of the invariant scheme of the method of fundamental solutions for two-dimensional potential problems in a Jordan region. Japan J. Indust. Appl. Math. **31**, 231–262 (2014)
20. Papkovich, P.F.: The representation of the general integral of the fundamental equations of elasticity theory in terms of harmonic functions (in Russian). Izv. Akad. Nauk. SSSR Ser. Mat. **10**, 1425–1435 (1932)
21. Pozrikidis, C.: Boundary integral and singularity methods for linearized viscous flows. Cambridge University Press, New-York (1992)
22. Schaback, R.: Error estimates and condition numbers for radial basis function interpolation. Adv. Comp. Math **3**, 251–264 (1995)
23. Sincich, E., Sarler, B.: Non-singular method of fundamental solutions based on Laplace decomposition for 2D Stokes flow problems. CMES Comput. Model. Eng. Sci. **99**(5), 393–415 (2014)
24. Tran-Cong, T., Blake, J.R.: General solutions of the Stokes' flow equations. J. Math. Anal. Appl. **90**(1), 72–84 (1982)
25. Tsai, C.C., Young, D.L., Fan, C.M., Chen, C.W.: MFS With time-dependent fundamental solutions for unsteady Stokes equations. Eng. Anal. Bound. Elem. **30**(10), 897–908 (2006)
26. Varnhorn, W.: Boundary value problems and integral equations for the stokes resolvent in bounded and exterior domains of $\mathbb{R}^n$, pp. 206–224. World Scientific Publishing, New York (1998)
27. Young, D.L., Lin, Y.C., Fan, C.M., Chiu, C.L.: The method of fundamental solutions for solving incompressible Navier-Stokes problems. Eng. Anal. Bound. Elem. **33**(8-9), 1031–1044 (2009)